Journal of Statistical Physics, Vol. 38, Nos. *3/4, 1985*

The Nonlinear Cahn–Hilliard Equation: Transition from Spinodal Decomposition to Nucleation Behavior

Amy Novick-Cohen[1]

Received August 3, 1983; revised July 3, 1984

The behavior of the nonlinear Cahn–Hilliard equation for asymmetric systems, $c_t = \nabla^2(\pm c + Bc^2 + c^3 - \nabla^2 c)$ within the unstable subspinodal region is explored. Energy considerations and amplitude equation methods are employed. Evidence is given for a transition from periodically structured"spinodal" behavior to nucleation behavior somewhere within the traditional spinodal. A mechanism for describing a time-dependent lengthening of the dominant wavelength is explored.

KEY WORDS: Phase separation; spinodal decomposition; nucleation; Cahn–Hilliard equation.

1. INTRODUCTION

Quenching (rapid cooling) of homogeneous binary systems, typically alloys,[1] glasses,[2] or polymers,[3] results in the separation of the system into two phases described by the "coexistence curve" concentrations; see Fig. 1. Traditionally, the path to phase separation is classified as either nucleation or spinodal decomposition. Shallow quenches, i.e., quenches from the stable region (point A) to some point just below the coexistence curve (point B), are said to proceed via nucleation, which roughly speaking is characterized by the random appearance of small "bubbles" of the minor phase c_2, which grow if sufficiently large, and which decay otherwise. On the other hand deep quenches from the point A to the point C below B are said to proceed via spinodal decomposition, which is characterized by the homogeneous onset of phase separation throughout the system. While

[1] Department of Applied Mathematics, The Weizmann Institute of Science, Rehovot, 76100 Israel. Present address: Institute for Mathematics and its Applications, 514 Vincent Hall, University of Minnesota, MPLS, MN 55455.

0022-4715/85/0200-0707$04.50/0

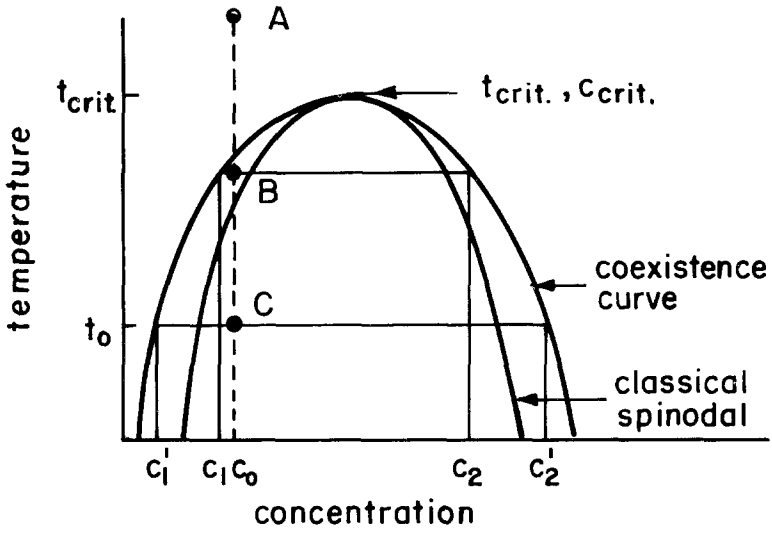

Fig. 1. Above the coexistence curve the system is stable; below it phase separation may occur. The highest temperature on the coexistence curve is known as T_{critical} and the corresponding concentration, c_{critical}. A system at concentration c_0 and temperature T_0 separates into the coexistence concentrations c_1 and c_2'. Conservation of matter determines the fraction at the total volume which appears in each of the two phases. The more distant of the two concentrations, c_2' becomes that of the minor phase. The inner line delineates the spinodal curve or the limit of linear stability of the one phase system.

experimentally[1] and theoretically[4,5] there does not appear to be a sharp crossover between nucleation and spinodal decomposition behavior, classically the crossover has been connected with the limit of linear stability which coincides with the locus of the inflexion concentrations of the free energy; see Fig. 2. Between the spinodal and the coexistence curve, a finite perturbation of the system is necessary to destabilize the system and cause phase separation. The coexistence curve is given by the locus of concentrations on a double tangent to the free energy; see Fig. 2. Such concentrations have identical chemical potential and may coexist. Beyond the coexistence curve, the only equilibrium state is the homogeneous one-phase state.

While nucleation theories date back to Becker and Doring[6] in 1935 and later Lifshitz and Slyozov[7] in 1961, the first attempt to treat spinodal decomposition was in 1958 via the phenomenological Cahn–Hilliard equation[8]

$$\frac{\partial c}{\partial t} = \nabla^2(f(c) + K\nabla^2 c) \tag{1.1}$$

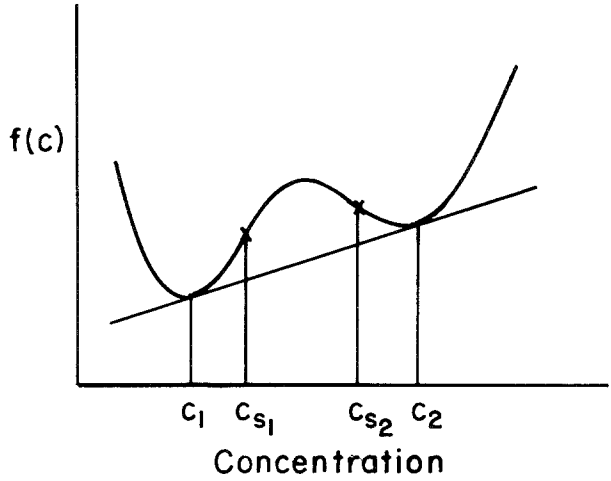

Fig. 2. The typical form of the free energy below the critical point, T_{crit}, c_{crit}. The coexistence concentration c_1 and c_2 correspond to the double tangent points of the free energy. The chemical potential $\mu = \partial f/\partial c$ is identical at the two coexistence concentrations. The overall free energy $F(c) = \int_v f(c)\, dV$ of a homogeneous system of concentration c_0, where $c_1 < c_0 < c_2$ is lowered by separation into these two concentrations. The spinodal curve of the limit of linear stability is given by the locus of those concentrations (c_{s_1}, c_{s_2}) where $\partial^2 f/\partial c^2$ vanishes. For homogeneous system of concentration $c_0, c_{s_1} < c_0 < c_{s_2}$, separation of the system into phases infinitesimally close to the original phase lowers the overall free energy.

where $c(x, t)$ is the concentration and $f(c)$ is the classical free energy. Early analysis of the Cahn–Hilliard equation was confined to the implications of the linear theory only.

We recall that linear stability analysis of the Cahn–Hilliard equation[16] predicts a fastest growing wavelength which diverges at the spinodal and whose amplitude is predicted to grow exponentially at earliest times (a prediction which reportedly has been verified[17]). The energy barrier, or equivalently the size of the perturbation which must occur in the system in order to initiate phase separation, is found (by linear analysis) to vanish within the spinodal region and is finite beyond it; thus it is not differentiable across the spinodal.[4] However it is well known that imperfections and impurities are capable of inducing a smoothed ("imperfect") bifurcation.[32]

In an attempt to remedy these nonphysical features predicted by linear analysis of the Cahn–Hilliard equation, various alternative methods of analysis were tried.[9–12] A common feature of these methods is the development of scaling predictions for the dynamics of nucleation and spinodal decomposition. In particular, the characteristic (or most dominant) wavelength of the system has been predicted[9,10,12] to behave at late times

as $at^{-\alpha}$, where the predicted value of α is method dependent, varying between approximately 0.19 and 0.35 and tending to be smaller at deeper quenches. Experiments in liquids[13] have provided evidence for the scaling laws, giving values of $\alpha \approx 0.33$. More recently the structure function

$$S(k,t) \equiv \int c(\mathbf{r}+r_0,t)\cdot c(r_0,t)\, e^{ik\cdot \mathbf{r}}\, d\mathbf{r}$$

has also been predicted[4,9,10,11a,14] to have a scaling form:

$$\bar{S}(k,t) = k_1^{-3} F(k, k_1(t)) \tag{1.2}$$

where

$$\bar{S}(k,t) = S \Big/ \int S^2(k,t)\, k^2\, dk$$

and where

$$k_1(t) = \int kS(k,t)\, dk$$

The scaling function $F(x)$ has been seen to be somewhat dependent on the location of the quenched state and tends to become more peaked at deeper quenches,[9] thus describing a smooth transition between spinodal and nucleation dynamics that has been reported elsewhere.[4,5]

While there are considerable differences between the predictions of Cahn–Hilliard theory (linear analysis) and those of other methods of analysis, it has been shown,[19] that the equations of Kawasaki dynamics reduce to Cahn–Hilliard theory when long-range interactions are considered. Thus, for example, in polymer systems where the interactions are inherently long range, the predictions of the various theories should coincide. See also Ref. 20 for a discussion of the convergence of classical and nonclassical spinodal behavior in the limit of long-range interaction systems. Clearly, stochastic driving forces are important in the evolution of the system and it would be most appropriate to consider the Cahn–Hilliard equation augmented by a stochastic driving force. Statistical approaches, however successful, always necessitate various approximating assumptions. The very past success of such approaches seems to justify a thorough study of the underlying *nonlinear* deterministic Cahn–Hilliard equation in order to ascertain what information is already contained there. Furthermore, we note that the Cahn–Hilliard equation has also appeared outside the context of spinodal decomposition,[21] and hence the study of the nonlinear Cahn–Hilliard equation is of some independent interest.

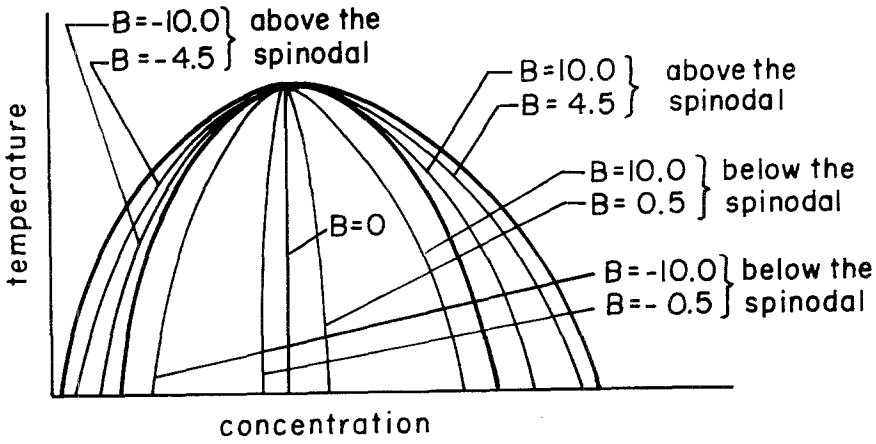

Fig. 3. The parameter B as a function of temperature and concentration.

Partial revelation of the full flavor of the nonlinear deterministic Cahn–Hilliard equation has appeared in Ref. 22. There the whole spectrum of the one-dimensional equilibrium solutions of the Cahn–Hilliard equation was presented [see also Eqs. (2.4), (2.5), below]. This was used in estimating the limit of monotonic global stability, or the limit beyond which all perturbations to the homogeneous state decay monotonically. This limit was shown to lie somewhere between the coexistence curve and a bounding line above it. The existence of an excitable region between the limit of monotonic global stability and the coexistence curve was conjectured. The existence of such an excitable region would be responsible for weak onset phenomena just beyond the coexistence curve. Furthermore, a finite amplitude periodic instability (in addition to the well-known nucleation instability) was shown to exist throughout the region beneath the coexistence curve.

It is of interest to ascertain what predictions may be made about the evolution of periodic structure within the context of the nonlinear deterministic Cahn–Hilliard equation. In approaching this problem, two difficulties are encountered. First, while there exist periodic stationary solutions, they are not stable in that they are not local minima of the free energy functional from which the Cahn–Hilliard equation is derivable. Secondly, spinodal decomposition occurs by bifurcation through zero wave number, hence the evolution of the fastest growing mode is highly influenced by the neighboring longer modes. In the present paper we show how two nonrigorous approaches may nevertheless provide some insight into the process of structural development. In Section 2 we see which stationary periodic solutions are admissible according to an energy criterion, and

compare their periods with the wavelength of the fastest growing mode. In Section 3, we study the growth of the shortest growing mode and use side band effects to take into account the other growing modes.

2. ADMISSIBLE STATIONARY SOLUTIONS

The Cahn–Hilliard equation can be derived from the Landau–Ginzburg free energy

$$F(c) = \frac{1}{V}\int_V [f(c) + K(\nabla c)^2]\, dv$$

by assuming the concentration flux to be proportional to minus the gradient of the first variation of $F(c)$. Then by conservation of matter,

$$\frac{\partial c}{\partial t} = \nabla(\mu(c)\, \nabla \delta F)$$

where $\mu(c)$ is the mobility. Here K and $\mu(c)$ are assumed to be positive. Writing the equation in dimensionless form for arbitrary perturbations c in the concentration about an initially uniform concentration, and assuming $f(c)$ to be a quartic polynomial in the concentration, we obtain

$$\frac{\partial c}{\partial t} = \nabla^2(\alpha c + Bc^2 + c^3 - \nabla^2 c) \tag{2.1}$$

In the same notation, the Landau–Ginzburg free energy is given by

$$F(c(x,t)) = \frac{1}{V}\int_V \left[\frac{1}{2}\alpha c^2 + \frac{1}{3}Bc^3 + \frac{1}{4}c^4 + \frac{1}{2}|\nabla c|^2\right] dv \tag{2.2}$$

Here α assumes the values ± 1, where $\alpha = 1$ refers to the thermodynamically stable and metastable regions denoted hereafter as the region above the spinodal, and where $\alpha = -1$ refers to the unstable region or the region below the spinodal. The parameter B is defined via derivatives of the free energy functional

$$B = \left(\frac{\partial^3 f}{\partial c^3}\right) \Big/ \left(\alpha \frac{\partial^2 f}{\partial c^2} \cdot \frac{\partial^4 f}{\partial c^4}\right)^{1/2}$$

where the derivatives are evaluated at the quench concentration c_0. Orientation with respect to the thermodynamic parameter B^2 is gained by noticing that if $\alpha = -1$, then $B^2 = 0$ at the critical quench concentration $(\partial^3 f/\partial c^3)(c_0 = 0)$ (see also Fig. 3). B^2 increases monotonically to infinity as

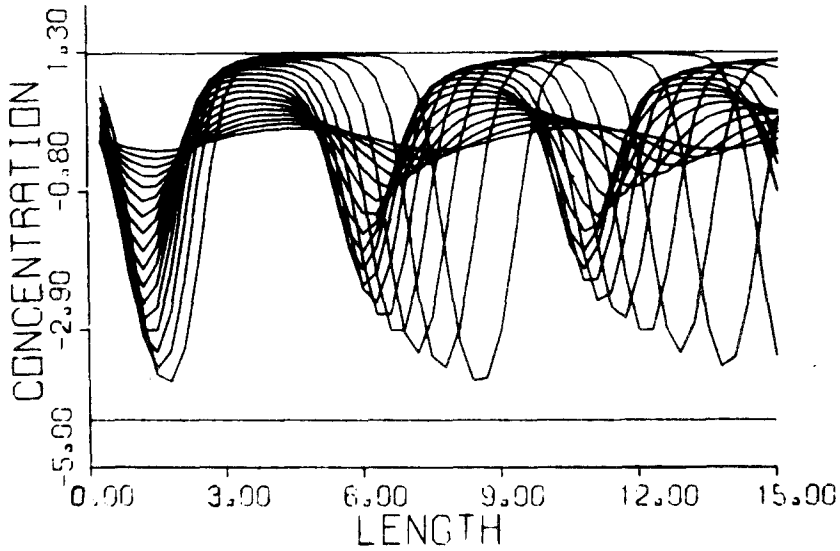

Fig. 4. Member of the class of one dimensional periodic equilibrium solutions at $B = 4.5$, below the spinodal.

the spinodal ($\partial^2 f/\partial c^2 = 0$) is approached. Beyond the spinodal ($\alpha = +1$), B^2 decreases until the value of 4.5 is assumed at the binodal (the double tangent to the free energy function). As a first approximation, the mobility and the coefficient of the surface energy contribution have been assumed to be constant, and have been subsumed into the time, length, and concentration scalings.

The results in this section as well as the next section hold both when the boundary conditions[22,25]

$$\nabla c = 0, \qquad \nabla(\nabla^2 c) = 0$$

are considered, as well as when periodic boundary conditions are assumed.

In examining the stability properties of the Cahn–Hilliard equation, we note that the free energy $F(c(x, t))$ acts as a Liapounov functional since[23]

$$\frac{\partial F(c(x, t))}{\partial t} \leqslant 0 \tag{2.3}$$

Furthermore, it is easy to see that all the equilibrium solutions of (2.1) are extremals of (2.2). Moreover, it can be shown that the class of equilibrium solutions consists of periodic solutions which are not local minima of the free energy,[26] and of a limiting "phase-separated" nonperiodic solution which attains global minima of the free energy.

Since we know the stationary solutions explicitly, it is easy to calculate their free energy and to ascertain which are admissible according to (2.3) from an initially slightly perturbed homogeneous state. Because the periodic solutions are not local minima, the justification for this calculation is not obvious. However, the justification appears *a posteriori*, in that more admissible solutions with periods similar to that of the fastest growing wavelength appear the closer we approach the critical concentration. It is then possible to conjecture that these stationary periodic solutions may serve as a series of saddles capable (locally in time) of stabilizing the transient periodic structure in the inner spinodal region.

The set of all one-dimensional equilibrium solutions of (2.1) is[22,25]

$$\psi(x;\lambda^2,B)=\frac{\beta_1(\gamma,\lambda^2)-\gamma^{1/2}\beta_2(\gamma,\lambda^2)\,sn(fx,\lambda^2)}{1-\gamma^{1/2}sn(fx,\lambda^2)} \tag{2.4}$$

where

$$\begin{pmatrix}\beta_1\\ \beta_2\end{pmatrix}=-\frac{1}{3}B\pm\begin{pmatrix}-2\gamma+1+\lambda^2\\ 2\dfrac{\lambda^2}{\gamma}-1-\lambda^2\end{pmatrix}\times\left[\frac{(1/3)B^2-\alpha}{(1+\lambda^2)^2-12\lambda^2+2(\lambda^2/\gamma+\gamma)(1+\lambda^2)}\right]^{1/2}$$

and where

$$f=\left[\frac{\alpha+B(\beta_1+\beta_2)+3\beta_1\beta_2}{2(1+\lambda^2)}\right]^{1/2}$$

Imposition of the composition conservation constraint, $\int_v c\,dv=0$, implies a functional dependence between γ and λ^2 which was obtained numerically in Refs. 22, 25. We note that for all values of B^2 for $\alpha=-1$, and for all $B^2>4.5$ for $\alpha=+1$, there exists a whole spectrum of solutions; see Fig. 4. Furthermore, for each (B,α), there exists a periodic equilibrium solution of smallest period. As the modulus $\lambda^2\to 1$, the periods increase and the solutions tend toward the nonperiodic "completely phase separated" solution

$$\psi(x,B^2)=-\frac{B}{3}+\left(\frac{B^2}{3}-\alpha\right)^{1/2}\tanh\left[\left(\frac{B^2}{3}-\alpha\right)^{1/2}-\frac{x}{2}\right] \tag{2.5}$$

We now use our knowledge of the functional dependence $\lambda^2=\lambda^2(\gamma)$ in order to calculate the free energies $F(c(\lambda^2;B))$ as a function of the modulus λ^2 for various values of the parameter B^2.

For convenience we normalize the free energy

$$\tilde{F}(c(x, t; B)) = -F(c(x, t; B))/F_{\min}(B) \tag{2.6}$$

where $F_{\min}(B) = -[B^2/9 - (1/2)\alpha]^2$ is the free energy of the completely phase separated solution in a limiting large system. Note that $\tilde{F}(c \equiv 0) = 0$. Hence if our initial state is a slight perturbation of a spatially homogeneous system, only those solutions whose free energies are negative are admissible according to (2.3).

The results of these calculations are portrayed in Fig. 5, where it can be seen that for all values of B^2 as $\lambda^2 \to 0$, the free energy of the equilibrium

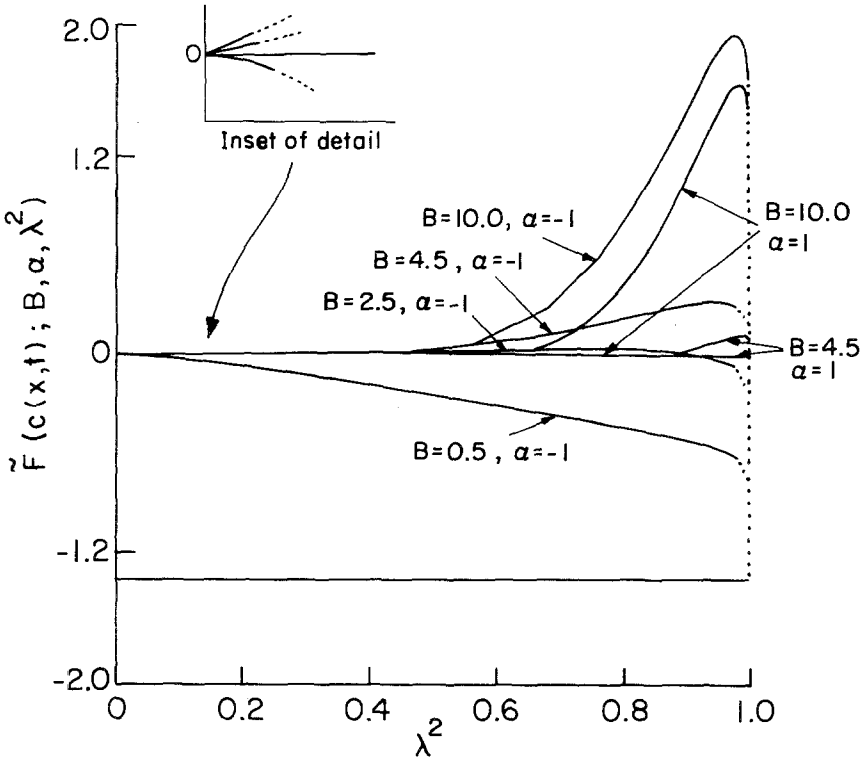

Fig. 5. For various values of the parameter B^2, the free energy of the equilibrium solutions has been portrayed as a function of the square of the Jacobian modulus λ. The free energy has been normalized here so that $\tilde{F}(c \equiv 0) \simeq 0$ and so that the free energy of the totally phase separated tanh solutions is -1. Since $dF/dt \leqslant 0$, all those solutions whose free energy is more than slightly greater than zero are unattainable by inducing small perturbations around the homogeneous state. The inset contains detailed sketch of the behavior of the free energy as a function of the square of the Jacobian parameter λ_1^2 for λ^2 small, and it can be seen that subspinodally, only for B^2 small is the free energy negative for equilibrium solutions for $\lambda^2 \ll 1$.

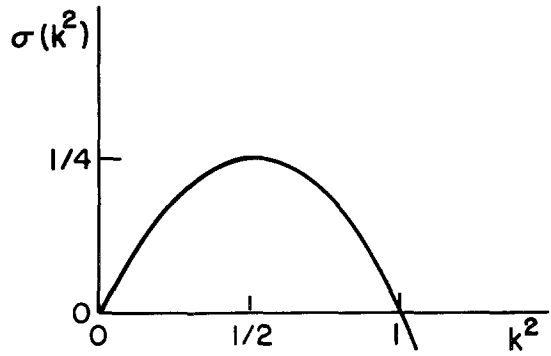

Fig. 6. The linear growth rate σ as a function of k^2. If we consider a length scale bifurcation then systems so small that the dimensions of the system $L < 2\pi$, are stable. A system whose dimensions are increased beyond 2π becomes unstable.

solutions approaches that of the spatially homogeneous state. From the asymptotics of the solutions,[22,25] we know that for all values of $B^2(\alpha = \pm 1)$, as $\lambda^2 \to 1$, the completely phase separated solution (2.5) is approached; hence it follows from (2.6) that for all (α, B) as $\lambda^2 \to 1$ the free energy approaches -1. In Fig. 5, this limiting behavior has been drawn in with a dotted line.

For $B^2 \ll 1(\alpha = -1)$ the free energy is negative for all values of λ^2 and decreases monotonically with λ^2 from an initial value of zero. For $B^2 \gg 1(\alpha = +1)$ the free energies of the equilibrium solutions are all positive until $\lambda^2 \approx 1$. In particular, for $B^2 \gg 1(\alpha = \pm 1)$ only those solutions for which $\lambda^2 \approx 1$ or $\lambda^2 \approx 0$ are conceivably attainable. Moreover, it is easy to show by asymptotic examination of the behavior of the amplitude of the equilibrium solutions (2.4) for all $B^2(\alpha = \pm 1)$, that $\lambda^2 = 0$ corresponds to the spatially degenerate homogeneous state $c \equiv 0$.

Thus it is clear from a preliminary glance at Fig. 5 that the set of λ^2 for which attainable configurations exist is much larger near $B^2 \approx 0$ and decreases with increasing B^2. We proceed now to compare the periods of these solutions with the length of fastest growing wavelength.

From the calculations on which Fig. 5 is based, it is known that for $B = 0.5(\alpha = -1)$ at $k^2 = 0.0082$ the free energy is already negative while for $B = 2.5(\alpha = -1)$, the free energy vanishes at some λ^2, $0.9110 < \lambda^2 < 0.9396$. By evaluating the period at these bounding values of λ^2 it is possible to obtain an estimate on the period of the configuration whose free energy vanishes; see Table I. For $B = 4.5$ and $B = 10.0$ the calculation of the free energy has been taken to values of λ^2 where the free energy is still very high. From (2.4), we see that the period is given by $T = 4K(\lambda^2)/f(\lambda^2, \gamma)$. The factor f^{-1} is nearly constant for $\lambda^2 \approx 1$ whereas $4K \to \infty$ as $\lambda^2 \to 1$. Lower

Table I. Estimates on the Period of That Nontrivial Solution Whose Free Energy Vanishes

B	α	k^2	Period
0.5	-1	$0 \leqslant k^2 < 0.0082$	$2\pi \leqslant K < 6.32$
2.5	-1	$0.9110 < k^2 < 0.9396$	$8.52 < L < 9.10$
4.5	-1	$0.978 < k^2 < 1.000$	$6.82 < L < \infty$
		$(0.00519)^a$	$(L > 8.37)$
10.0	-1	$0.997 < k^2 < 1.000$	$4.18 < L < \infty$
		(0.999968)	$(L > 6.38)$

[a] The values in parentheses correspond to interpolated estimates.

bounds are obtained by evaluating the period at the last value of k^2 evaluated or alternatively at a value λ^2 obtained by linear interpolation between the last value calculated and $\lambda^2 = 1$; see Table I. Clearly the decay in the free energy appears from Fig. 5 to be steeper than linear, hence the periods can be expected to be longer than the estimate in parenthesis.

Thus we see that for $B^2 \approx 0$ there are solutions with $\lambda^2 \approx 0$ whose free energy is just slightly less than that of the spatially homogeneous solution and whose period is very similar in size to the wavelength of the fastest growing mode, 2π.

On the other hand when $B^2 \gg 1$ only those solutions for which $\lambda^2 \approx 1$ are conceivably attainable. In particular we see that the class of attainable solutions is larger for the near critical region than elsewhere, and that within this internal region there exist admissible equilibrium solutions whose period is similar in size to the wavelength of the fastest growing mode of linear stability.

3. AMPLITUDE EQUATION METHOD

In the previous section, we saw that the distribution of the free energies of the equilibrium solutions was considerably different for the region $B^2 \ll 1 (\alpha = -1)$, i.e., in the region near the critical concentration, than elsewhere. In this section, we analyze the evolution of a single mode located at the short wavelength end of the spectrum of growing modes in order to model the development of finite amplitude periodic structure from an initially imposed infinitesimal perturbation around a spatially homogeneous state. This approach is shown capable of describing the evolution of periodic structure in the region near the critical concentration. Thus the results of Sections 2 and 3 suggest that phase separation in the deep spinodal region

may be distinguishable, perhaps more nearly periodic or "spinodal," than in the rest of the spinodal region. Again, the mobility and the coefficient of the surface energy contribution are assumed to be constant.

3.1. The Amplitude Equations

Since we are in the deep unstable region, the growth rate of the fastest growing mode is in fact $O(1)$ (except in the direct neighborhood of the spinodal) and it is not possible to use conventional nonlinear stability theory[28] to develop amplitude equations for the fastest growing mode. However, modes near the critical wavelength (the longest growing wavelength, $k_c^2 = k_{\max}^2/2$) grow more slowly and amplitude equations in terms of these modes are readily obtained. Thus it is possible to first study the evolution of this mode and later to account for effects of the longer growing modes by including an additional long length scale.

This approach would be fully justified if it could be demonstrated that in some system the shorter growing modes are initially more frequent in the system than the other growing modes. Strictly speaking, examination of the smallest growing modes corresponds to consideration of a length scale bifurcation (see Fig. 6), i.e., to considering a system whose size has been limited to only a few times the wavelength of the fastest growing mode. This would correspond to looking at a system whose dimensions are of several tens of angstroms in the case of binary alloy systems to several hundreds of angstroms in the case of phase separation in polymer systems. It may, in fact, be technically feasible to carry out such experiments if the resultant system is large enough to overcome edge effects.[27]. We may consider our approach to describe a particular subset of all possible evolutions, whose results may or may not be fully applicable to the more general case. Some analysis of the behavior of the smallest growing mode has already appeared in the context of spinodal decomposition.[19] We note that externally forced systems do lend themselves to traditional amplitude equation methods.[33]

Amplitude equations for the mode $k^2 = 1 - \rho\varepsilon^2 (k_c^2 = 1$; Ref. 25) may be obtained by introducing the expansion $c = \sum \varepsilon^i c_i$, where $\varepsilon^2 \equiv \| c^2(0) \| L_2$ and by defining the slow time variable $\tau = \varepsilon t$. It is then possible to prescribe the following hierarchy of $O(\varepsilon^i)$ equations:

$$L_i \equiv -\nabla^2(-(1-\rho\varepsilon^2)\, c_i - \nabla^2 c_i) \tag{3.1}$$

$L_i = N_i$ [all nonlinear terms of size $O(\varepsilon^i)$], $i \geqslant 1$, where the solution is required to be periodic. The amplitude equations are then obtained by sequential solution of the first few equations and by elimination of resonant terms. Transient effects which have not been explicitly considered here are in

fact readily taken into account[29] by the inclusion of an additional, fast, time scale.

If we constrain ourselves temporarily to one dimension we obtain the "roll" amplitude equation

$$\frac{d}{d\tau}A = k^2 A + \left[\frac{2B^2}{3} - 3k^2\right]|A|^2 A \tag{3.2}$$

for solutions at lowest order which are of the form $c_1 = A(r)^{ikx} + \bar{A}(r)\,e^{-ikx}$. Likewise, if we assume that $B = O(\varepsilon)$, consideration of two dimensional perturbations leads to the amplitude equations

$$\begin{aligned}\frac{d}{d\tau}(2X) &= -k^2\left[-\rho X + 2BXY + \left(\frac{9}{2} + 3XY^2\right)\right]\\ \frac{d}{d\tau}(Y) &= k^2\left[-\rho Y + BX^2 + \left(\frac{3}{4}Y^3 + 3X^2Y\right)\right]\end{aligned} \tag{3.3}$$

for "hexagonal" solutions of the form (at lowest order)[28]

$$c_1 = 2X(\tau)\cos\left(\frac{\sqrt{3}}{2}kx\right)\cos\left(\frac{1}{2}ky\right) + Y(\tau)\cos(ky)$$

In one dimension there exists a steady state solution which is stable within the framework of equation (3.1) if $B^2 < \frac{9}{2}k^2$. Thus if B^2 is sufficiently small it is possible in one dimension to follow the development of an infinitesimal perturbation toward a periodic stationary state.

Similarly, in two dimensions, the nontrivial steady state solutions to (3.3) are given by

$$\begin{aligned}&\mathrm{I}_{\pm}: && X = 0, && Y = \pm(\tfrac{4}{3}\rho)^{1/2}\\ &\mathrm{II}_{\pm}: && Y = -\tfrac{4}{3}\bar{B}, && X = \pm(\tfrac{4}{9}\rho - \tfrac{16}{27}\bar{B}^2)\\ &\mathrm{III}_{\pm}: && X = Y, && Y = \tfrac{2}{15}[-\bar{B} \pm (\bar{B}^2 + 15\rho)^{1/2}]\\ &\mathrm{IV}_{\pm}: && X = -Y, && Y = \tfrac{2}{15}[-\bar{B} \pm (\bar{B}^2 + 15\rho)^{1/2}]\end{aligned} \tag{3.4}$$

Note first that case I_+ corresponds to the one-dimensional solution mentioned above. Within the framework of system (3.3), assuming $\rho > 0$, the trivial solution is always unstable (as predicted by linear stability) and I_+ is always stable as it was within the context of Eq. (3.2). On the other hand I_- is stable only if $\bar{B}^2 < \frac{3}{56}\rho$. In cases III and IV, in each set one of the two solutions is always unstable, whereas if $\bar{B}^2 > \frac{3}{16}\rho$ the remaining solution is stable. Thus if $\bar{B} = O(\varepsilon)$, there exist stable roll solutions (case I), if $\bar{B}^2$ is sufficiently small there exist stable rectangular solutions (case II), and for $\bar{B}^2$

sufficiently large exist stable hexagon solutions (cases III and IV). Since the analysis has been strictly based on the assumption that $B = O(\varepsilon)$, there is no reason to conclude that the hexagon solutions remain stable as B becomes $O(1)$.

3.2. Side Band Effects

It is possible to see how the growth of a solitary mode on the short end of the spectrum of growing modes is affected by the other growing modes by including an additional long spatial scale $x_2 = \varepsilon^2 x$ in the analysis carried out above. This approach is similar to the standard method of including side band[30] around the fastest growing mode, except that here the side bands are all on one side of the mode under consideration.

The resultant equation in one dimension is

$$\frac{\partial A}{\partial \tau} = k^2 \rho A + \left[\frac{2B^2}{3} - 3k^2\right] |A|^2 A - 2(1-k^2)\, ik \frac{\partial A}{\partial x_2} \tag{3.5}$$

It is possible to use Eq. (3.5) to test the stability of the steady state solutions of (3.2) to long wavelength perturbations by imposing $A = (k^2\rho[2B^2/3 - 3k^2]^{-1})^{1/2} + \varepsilon a(x_2, \tau)$ as an initially perturbed, initial condition.

Doing so, we find that the solutions are indeed unstable to long wavelength perturbations, and apparently give rise to gradual variation of the dominant wavelength. It would be interesting to study the time dependence of the variation of the dominant wavelength. This could serve as a basis for comparison with the scaling laws described in Section 1.

3.3. Transitional Behavior

In order to obtain a glimpse into the transitional behavior between the inner spinodal region where there appears to exist the possibility of a smooth path to a periodic (although, according to Section 2 most probably an unstable) solution and the outlying region in which this possibility no longer exists, we examine the behavior at the edge of this inner region, in the one-dimensional case, by expanding the parameter B^2 about the value $B^2 = 4.5k^2$. Thus we set $B^2 = 4.5k^2(1+\delta^2)$, $k^2 = 1 - \rho\delta$, $s = \delta^4 t$, and we construct an asymptotic expansion $c = \delta c_1(x, s) + \delta^2 c_2(x, s) + \cdots$. As before a solution of the form $c_1 = G(s)\, e^{ikx} + \bar{G}(s) e^{-ikx}$ is obtained, and at fifth order, the solvability condition yields the amplitude equation

$$\frac{d}{ds} G = \rho G + 3\,|G|^2\, G - 3\,|G|^4\, G \tag{3.6}$$

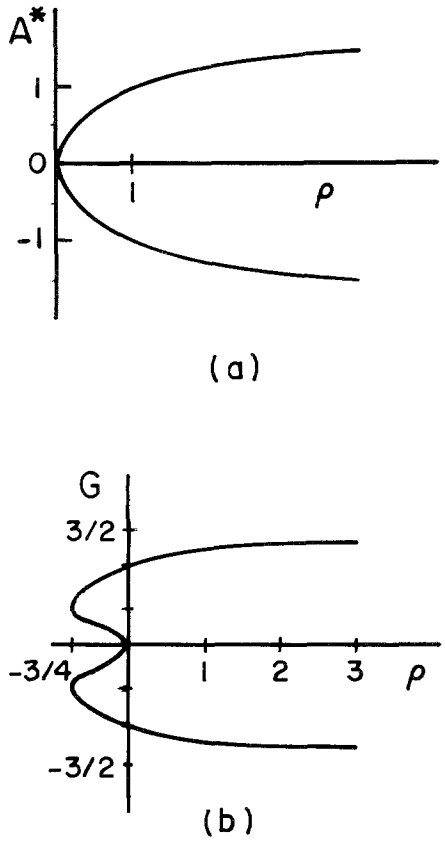

Fig. 7. The amplitude of the roll solution. In (a), $A^* = A/(3/2 - B^2/3)$, and it is assumed that $B^2/3 < 3/2$. The bifurcation parameter is given by $\rho = (1 - k^2)/\varepsilon^2$, where $\varepsilon^2 \equiv \|c^2(0)\|$. In (b), $2B/9 - 1 = \delta^2$ and $\rho = (1 - k^2)\,\delta^{-4}$, where $\delta^2 = \|c^2(0)\|$.

As noted by Sivashinsky,[31] this is precisely the form of an equation expected to model subcritical bifurcation (here in terms of the length scale); see Fig. 7. This would indicate that perturbations of length scale even smaller than 2π would be capable of destabilizing the system. This would correspond to a transition from a region within which the path to the final state is smooth (or begins smoothly) to a region within which the system jumps in a very highly perturbation-dependent manner. Such a transition is precisely what would be expected to be seen in a transition from the spinodal region to the nucleation region.

4. CONCLUSION

We have tried to demonstrate those features of spinodal decomposition and nucleation which are obtainable by study of the nonlinear Cahn–Hilliard equation without reference to a specific noise source.

First, evidence is given for a smooth transition from spinodal decomposition to nucleation somewhere within the classical spinodal. This is seen by noting that the energetically admissible solutions (which are not in fact local minima) with period of the size of the fastest growing mode are more frequent within the deep spinodal region than elsewhere. Furthermore we have shown by considering the growth of the critical growing wavelength, that hexagon solutions are possible in a region sufficiently close to the critical concentration, and that roll solutions are possible within a considerably larger subspinodal region, and not beyond. At the edge of the region where rolls are possible a transition from subcritical to supercritical bifurcation takes place which would be reminiscent of a smooth transition from spinodal decomposition to nucleation and growth.

Secondly, by considering side band effects, a mechanism for describing the lengthening of the dominant mode is shown to be a consequence the Cahn–Hilliard equation.

Thus while the Cahn–Hilliard equation cannot be considered to contain all the information contained in a full noise driven approximation, we feel that we have demonstrated here that the theory is considerably richer than would be predicted from linear theory only.

ACKNOWLEDGMENT

I wish to thank L. A. Segel and H. L. Frisch for reading and commenting on early drafts of this paper.

5. REFERENCES

1. B. Rundman and J. E. Hilliard, *Acta Metallurgica* **15**:1025 (1967); V. Gerald and J. Kostartz, *J. Appl. Cryst.* **11**:376 (1978).
2. *Discuss. Faraday Soc.* **50** (1971).
3. C. A. Smolders, J.J. van Aartsen, and A. Steenbergen, *Kolloid-Z. Z, Polymers* **243**:14 (1971).
4. K. Binder, C. Billotet, and P. Mirold, *Z. Phys.* **B30**:183 (1978).
5. J. L. Lebowitz, J. Marro, and M. H. Kalos, *Comm. on Solid State Phys.* (1982).
6. R. Becker and W. Doring, *Ann. Phys.* (*Leipzig*) **24**:719 (1935).
7. J. M. Lifshitz and V. V. Slyozov, *J. Phys. Chem. Solids* **19**:35 (1961).
8. J. W. Cahn and J. E. Hilliard, *J. Chem. Phys.* **28**:258 (1958).

9. (a) J. Marro, J. Lebowitz, and M. Kalos, *Phys. Rev. Lett.* **43**:282 (1979); (b) J. L. Lebowitz, J. Marro, and H. H. Kalos, *Acta Metallurgica*, **30**:297 (1982), and references therein.
10. K. Binder and D. Stauffer, *Phys. Rev. Lett.* **33**:1006 (1974).
11. (a) K. Binder, *Phys. Rev.* **B15**:4425 (1977); (b) K. Binder and D. Stauffer, *Adv. Phys.* **25**:343 (1976).
12. J. S. Langer, M. Bar-on, and H. D. Miller, *Phys. Rev. A* **11**:1417 (1975).
13. (a) Y. C. Chou and W. I. Goldburg, *Phys. Rev. A* **23**:858 (1981); (b) N. C. Wong and C. M. Knobler, *Phys. Rev. Lett.* **43**:1733 (1979).
14. M. Furukawa, *Phys. Rev. Lett.* **43**:136 (1979).
15. (a) N. C. Wong and C. M. Knobler, *J. Chem. Phys.* **69**:725 (1978); (b) Y. C. Chou and W. I. Goldburg, *Phys. Rev.* **A20**:2105 (1979).
16. J. W. Cahn, *Trans. A.I.M.E.* **242**:166 (1968).
17. M. R. Murzik, F. F. Abraham, and G. M. Pound, *J. Chem. Phys.* **69**:3462 (1978).
18. A. B. Bortz, *J. Stat. Phys.* **11**:181 (1974).
19. K. Binder, *Z. Phys.* **267**:313 (1974).
20. D. W. Heermann, W. Klein, and D. Stauffer, *Phys. Rev. Lett.* **49**:1267 (1982).
21. J. K. Percus and S. Childress, Mathematical Models in Developmental Biology (Lecture Notes), Courant Institute, New York (1978), Chap. 21; (b) D. S. Cohen and J. D. Murray, *J. Math. Bio.* **12**:237 (1981); (c) A. C. Brown, C. Unger, and W. Klein, *Z. Phys.* **B48**:1 (1981).
22. A. Novick-Cohen and L. A. Segel, *Physica* **10D**:277 (1984).
23. J. S. Langer, *Ann. Phys. (N.Y.)* **65**:53 (1971).
24. D. DeFontaine, Ph.D. thesis (Northwestern University, Evanston, Illinois, 1967).
25. A. Novick-Cohen, Ph.D. thesis (Department of Applied Mathematics, Weizmann Institute of Science, Rehovot, Israel, 1982).
26. J. Carr, M. Gurtin, and M. Slemrod, *Arch. Rat. Mech. Anal.*, to appear.
27. Y. Imry, *Phys. Rev. B* **21**:2042 (1980).
28. L. A. Segel, in *Non-Equilibrium Thermodynamics—Variational Technique and Stability*, R. J. Donnelly, ed. (Chicago University Press, Chicago, 1966), p. 165.
29. J. B. Matkowsky, *SIAM J. Appl. Math.* **18**:872 (1970).
30. J. T. Stuart and R. C. DiPrima, *Proc. R. Soc. London Ser. A* **362**:(1978).
31. V. L. Gertzberg and G. I. Sivashinsky, *Prog. Theor. Phys.* **66**:1219 (1981).
32. B. J. Matkowsky and E. L. Reiss, *SIAM J. Appl. Math.* **33**:(1977).
33. E. Coutsias and B. A. Huberman, *Phys. Rev. B* **24**:2592 (1981).